Polymer Bulletin (2019) 76:3535–3554
https://doi.org/10.1007/s00289-018-2557-x

ORIGINAL PAPER

Cross-linking and modification of sodium alginate biopolymer for dye removal in aqueous solution

Akila Merakchi[1,2] · Souhila Bettayeb[2,3] · Nadjib Drouiche[4] · Lydia Adour[5] · Hakim Lounici[2,6]

Received: 30 July 2018 / Revised: 26 September 2018 / Accepted: 6 October 2018 /
Published online: 15 October 2018

Abstract

In this study, spherical beads have been prepared by ionotropic gelation of sodium alginate using two types of cross-linking, physical cross-linking in the presence of Ca^{2+} ions and chemical cross-linking which was made with epichlorohydrin for environmental applications. The different beads of alginate were characterized by Fourier transform infrared spectroscopy, optical microscopy, scanning electron microscopy, and X-ray diffractometry to provide evidence of successful cross-linking. The physicochemical properties of the beads such as the average diameter, water content, the zero charge point, and the density were also determined. The efficiency of the beads as biosorbent for the removal of dyes is assessed using methyl violet (MV) as a model molecule. A comparative adsorption performance of wet calcium alginate beads (WCaAB), dry calcium alginate beads (DCaAB), wet epichlorohydrin cross-linked alginate beads (WEpAB), and dry epichlorohydrin cross-linked alginate beads (DEpAB) was made. The adsorption of methyl violet MV on cross-linked alginate beads was found to be comparatively higher than that of WCaAB, DCaAB, and WEpAB. The extent of adsorption of methyl violet MV onto cross-linked alginate beads (DEpAB) was found to be a function of the pH of the solution, contact time, sorbate concentration, amount of beads and stirring speed. The kinetics adsorption of MV onto cross-linked alginate beads (DEpAB) was investigated using the pseudo-first-order, pseudo-second-order, and intraparticle diffusion kinetic models. The results showed that the pseudo-second-order kinetic model adequately describes the experimental data.

Keywords Biopolymer · Sodium alginate · Cross-linking · Epichlorohydrin · Alginate beads · Adsorption · Methyl violet

✉ Hakim Lounici
hakim_lounici@yahoo.ca; nadjibdrouiche@yahoo.fr

Extended author information available on the last page of the article

Introduction

Human health, water quality, and aquatic life are directly or indirectly affected by industrial effluents when these effluents are released into aquatic environments [1, 2]. This pollution has adverse effects on living organisms, on the self-cleaning power of water, and leads to the accumulation of certain harmful elements in the food chain.

Textile and dyeing industries contribute significantly to environmental contamination. It is widely accepted that dyes are currently widely used in the textile, paper, food, beverage, pharmacy and leather industries [3–5]. Dyes are synthetic organic compounds capable of producing or generating active substances that are often non-biodegradable [6]. It is also known that a small amount of even tiny dye present in the water can generate color in the bulk and make it unusable. Various treatment technologies like adsorption [7–11], photodegradation [12–16], coagulation–flocculation [17], chemical oxidation [18, 19], electrochemical techniques [20, 21], biological process [22], precipitation [23], membrane filtration [24] exist and therefore available for the treatment of colored wastewater. Among these approaches, adsorption is regarded as an easy, economical, and desirable process, due to efficiency and ability to eliminate a wide range of pollutants from industrial effluents [25].

Recently, many natural biopolymer adsorbents, such as sodium alginate, chitosan, and guar gum, have been attractive as they are efficient, inexpensive, non-toxic, biodegradable, and environmental friendly [26–28]. Among the polymers of biological origin, alginate is one of the most studied biomaterials for the removal of pollutants from aqueous solutions. It is a natural product; it is now recognized as an unbranched anionic copolymer composed of two monomers units (1–4) linked β-D-mannuronic acid (M) and α-L-guluronic acid (G) and is extracted from brown algae constitutes. The sodium alginate is water soluble and less stable, and hence it cannot be used for adsorption process directly. In order to overcome this difficulty, one of the attempts used is the cross-linking to increase its stability and sorption capacity.

Therefore, various physical and chemical modifications have been developed to increase the chemical stability sodium alginate for use as cleaning agent for depollution, but these beads present defects such as crumbling or non-stability that would pose problems when used in water treatment.

In the present work, sodium alginate was cross-linked physically with calcium ions and chemically using epichlorohydrin as a cross-linking agent, to prepare an innate adsorbent, alginate beads, which have been used for removal of the methyl violet dye of an aqueous solution under various operating conditions. The insertion of epichlorohydrin as a cross-linking agent is already used to obtain beads in other uses but to our knowledge not yet used as a cleaning agent.

In addition, we were interested in the use of beads in wet and dry form; the latter form would have certain advantages in their use and conditioning and will give some potential in their use in dynamic mode.

Experimental

Materials

- Sodium alginate powder low viscosity (viscosity of 1% w/v solution at 25 °C: 5.5 ± 2.0 Cps) was purchased from Biochem Chemopharma and used as received.
- Calcium solutions were prepared by dissolving a known quantity of calcium chloride dihydrate (Fluka) in distilled water.
- Epichlorohydrin (3-chloro-1,2-epoxypropane) with a purity of 99% was purchased from Biochem Chemopharma.
- The dye methyl violet (noted VM) was purchased from Biochem Chemopharma.

Methods

Preparation of calcium alginate beads

Four grams of sodium alginate powder was dissolved in 100 mL of distilled water with stirring until the solution become homogenous. For the preparation of the beads, the polymer solution was added dropwise in a calcium bath (400 mL/0.3 mol L^{-1}) using a 5-mL hypodermic syringe under constant stirring at room temperature. The beads, thus formed, were cured in the calcium bath for 24 h, so this time is necessary to ensure that the gelling reaction has proceeded entirely throughout the volume of the beads. After the curing period, the beads were washed several times with distilled water bath to remove the maximum amount of unbound calcium. The weight of wet beads for a typical preparation is 200 ± 5 g. After their synthesis, the calcium alginate beads can be used directly, and they are then called wet calcium alginate beads (WCaAB), or were dried by exchanging the water in the gel with ethanol followed by drying in an air stream and dried in an oven at 60 °C for 24 h and become dry (DCaAB) [29–31]. Figure 1 shows photographs of the products obtained.

Preparation of epichlorohydrin cross-linked alginate beads

Epichlorohydrin-reticulated alginate beads (EpAB) were prepared starting from calcium alginate beads (method described in the section "Preparation of calcium alginate beads"). Chemically cross-linked alginate beads were obtained following a procedure adapted from [32–34]. First, 186 ± 2 g of WCaAB was immersed into three consecutive ethanol/water baths (60% v/v in ethanol, 400 mL each) during 2 h each to exchange the water contained in the beads with ethanol. The beads were then put into 400 mL of an ethanol/water solution (60% v/v of ethanol) containing epichlorohydrin (6109 g), to reach pH ≈ 13; NaOH solution (1 M) was then slowly added. The cross-linking reaction was allowed to proceed for 4 h. The beads were then washed in three repeated distilled water baths (600 mL each for 2 h). The concentrated HNO_3 solution was added to the last bath to neutralize the mixture

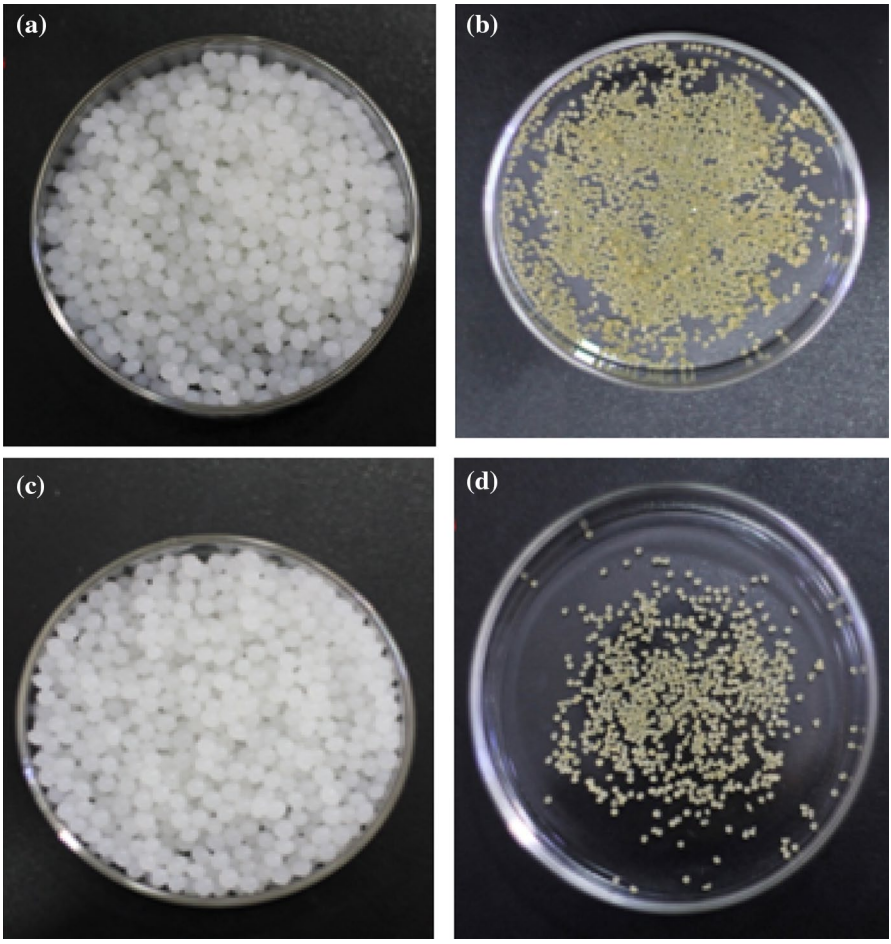

Fig. 1 Photographs of beads. **a** Wet calcium alginate beads (WCaAB). **b** Dried alginate beads (DCaAB). **c** Wet epichlorohydrin cross-linked alginate beads (WEpAB) and **d** dried epichlorohydrin cross-linked alginate beads (DEpAB)

(pH ≈ 7). The beads were collected afterward and were used either wet (WEpAB) or dry (DEpAB).

Characterization of beads

The average diameter of beads was obtained using a digital caliper device. For accurate results, diameter measurement was performed for more than 440 wet alginate beads and 250 dry alginate beads.

The apparent density of different beads was determined according to the gravimetric method.

All beads were dried at 105 °C until constant mass, and water content could be calculated using the following formula:

$$W(\%) = \frac{W_w - W_d}{W_w} \times 100 \quad (1)$$

where W_w and W_d represent the mass (g) of the wet and dried samples, respectively.

The pH of the point of zero charge (pH_{pzc}) of beads was measured using the pH drift method [35]. To a series of bottles of 100 mL, 50 mL of distilled water was added and initial pH_i was adjusted from 2 to 12 with 0.1 M HCl OR 0.1 M NaOH solutions. To the adjusted pH solution, 0.15 g of beads was added and the suspensions were shaken manually and allowed to equilibrate for 48 h. After 48 h, the suspensions were separated by filtration, and the pH_f values of supernatant liquid were noted. The figure of pH_{final} versus $pH_{initial}$ was used to determine the point at which $pH_{initial}$ and pH_{final} values were equal. This point was taken as pH_{pzc}.

Fourier transform infrared (FTIR) spectroscopy was used to confirm the presence of functional groups in samples, and the FTIR spectra of different beads were recorded in an FTIR spectrometer (JASCO FT/IR-4200, ATR PRO450-S) over the wave range 4000–400 cm^{-1}, at spectral resolution of 4 cm^{-1}. All the samples were crushed with potassium bromide to get pellets at 600 kg cm^{-2}.

The morphology and surface structure of the beads was examined by scanning microscope (Quanta 650) and optical microscope (Leica). The beads were also subjected to characterization using X-ray fluorescence (PANalytical Epsilon 3-XL).

Batch-mode adsorption studies

Batch adsorption experiments were conducted at room temperature. The effects of the experimental parameters such as the nature of the beads (WCaAB, WEpAB, DCaAB, and DEpAB), the contact time (0–5 h), initial dye concentration (10–70 mg L^{-1}), amount of adsorbent (DEpAB) 0.25–2.5 g, solution pH (3–10), and stirring speed (100–700 rpm) is studied in batch mode for a specific period of contact time. The experiments were conducted at 22 °C (room temperature).

A series of 400-mL Erlenmeyer flasks were filled with exactly 100 mL of dye (VM) solution of known initial concentration and stirred at a known speed. After reaching equilibrium, the residue concentrations of dye were determined by spectrophotometer (JENWY 6850) at a maximum wavelength of 582 nm. Percentage removal (R (%)) and the adsorption capacities (Q_t) of MV at any time were calculated according to the following equations:

$$R(\%) = \frac{(C_0 - C_t)}{C_0} \times 100 \quad (2)$$

$$Q_t = \frac{(C_0 - C_t) \times V}{w} \quad (3)$$

where Q_t is the adsorption capacity (mg g^{-1}), R (%) the percentage dye removal, C_0 and C_t the initial and residual dye concentrations in the solution (mg L^{-1}), V the solution volume (L), and W the amount of adsorbent (g).

Adsorption kinetics

The kinetic study is important for the adsorption process because it describes the uptake rate of adsorbate and controls the residual time of the whole process. The adsorption of MV onto beads was analyzed using both pseudo-first-order and the pseudo-second-order kinetic models. The pseudo-first-order equation can be expressed as:

$$\frac{dQ_t}{dt} = k_1\left(Q_e - Q_t\right) \tag{4}$$

where Q_e represent the amount of MV adsorbed at equilibrium (mg g^{-1}), Q_t the amount of MV adsorbed at time t (mg g^{-1}), k_1 the rate constant for pseudo-first order adsorption (min^{-1}).

After integration and application of boundary conditions using initial conditions, such as $(Q_e - Q_t) = 0$ at $t = 0$, the equation becomes:

$$\log\left(Q_e - Q_t\right) = \log Q_e - \frac{k_1}{2.303}t \tag{5}$$

The formula for pseudo-second-order kinetics is generally employed in the form proposed by Ho and Mckay [36] as:

$$\frac{dQ_t}{dt} = k_2\left(Q_e - Q_t\right)^2 \tag{6}$$

In which k_2 is the pseudo-second order kinetic rate constant (g mg^{-1} min^{-1}).

The following linear form for a pseudo-second-order reaction equation can be expressed as follows:

$$\frac{t}{Q_t} = \frac{t}{Q_e} + \frac{1}{k_2 \cdot Q_e^2} \tag{7}$$

The experimental data were also analyzed by running the intraparticle diffusion kinetic model, in order to identify the steps involved during adsorption. The kinetic model (according to the Weber–Morris model) is described by both external mass transfer and intraparticle diffusion, thus yielding Q versus the square root of time $t^{1/2}$. The linear form of this intraparticle diffusion model equation can be expressed as follows [37]:

$$Q = k_d t^{1/2} + L \tag{8}$$

where k_d (mg g^{-1} $min^{-1/2}$) is the intraparticle diffusion rate constant, the values of L (mg g^{-1}) provide an idea about the initial portion of MV that attaches onto the beads surface.

Results and discussion

Beads formation and characterization

The formation of beads takes place due to ionotropic gelation of spherical drops Ca^{2+} ions in the case of the calcium alginate beads. The polyguluronate units in the alginate molecules form a chelate structure with metal ions, called an "egg-box" junction with interstices in which the cations may pack and be coordinated. The junctions between the chains formed in this way are kinetically stable toward dissociation, while the polymannuronate units show the normal polyelectrolyte characteristics of cations binding [38]. The two interactions as represented in Fig. 2 thus resulting in the formation of spherical beads.

When epichlorohydrin is used as a cross-linking agent, the formation of the gel alginate is slower than with calcium ions, so we cannot directly form beads. This difficulty is usually circumvented by preparing in firstly calcium alginate beads and then cross-linking with epichlorohydrine in a second time [39]. The cross-linking reaction of alginate by a molecule of epichlorohydrin from calcium alginate is shown in Fig. 3.

The size distribution curves of different alginate beads tend to fit the Gaussian distribution (Fig. 4), and also the average size and the polydispersity factor of

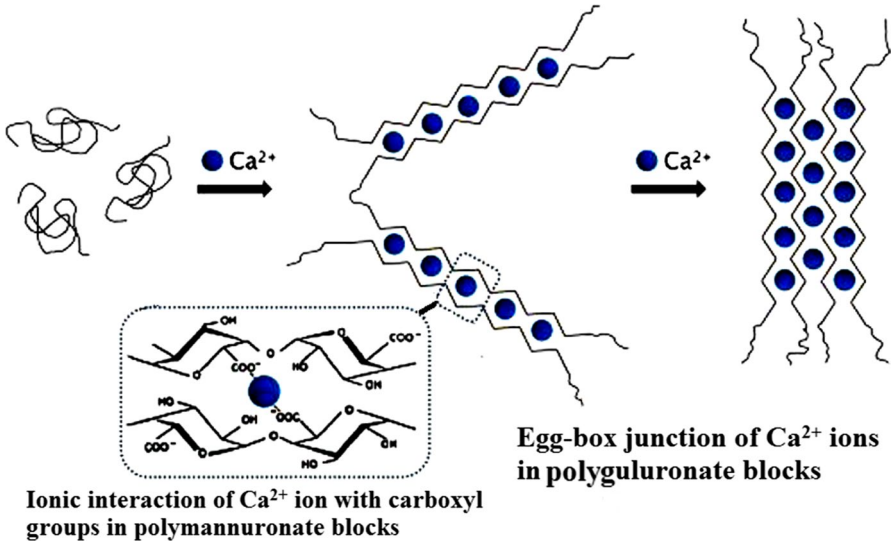

Fig. 2 Bonding interactions between Ca^{2+} ions and $–COO^-$ group in the calcium alginate beads

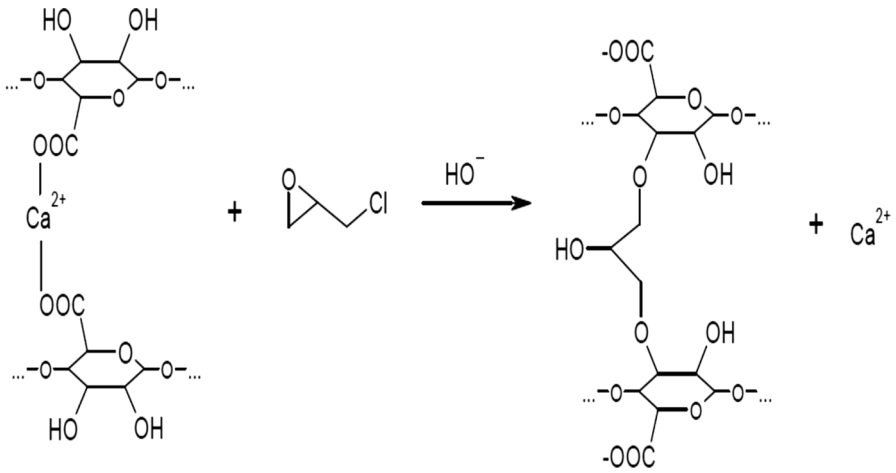

Fig. 3 Alginate cross-linking reaction by epichlorohydrin Reproduced with permission from [39]

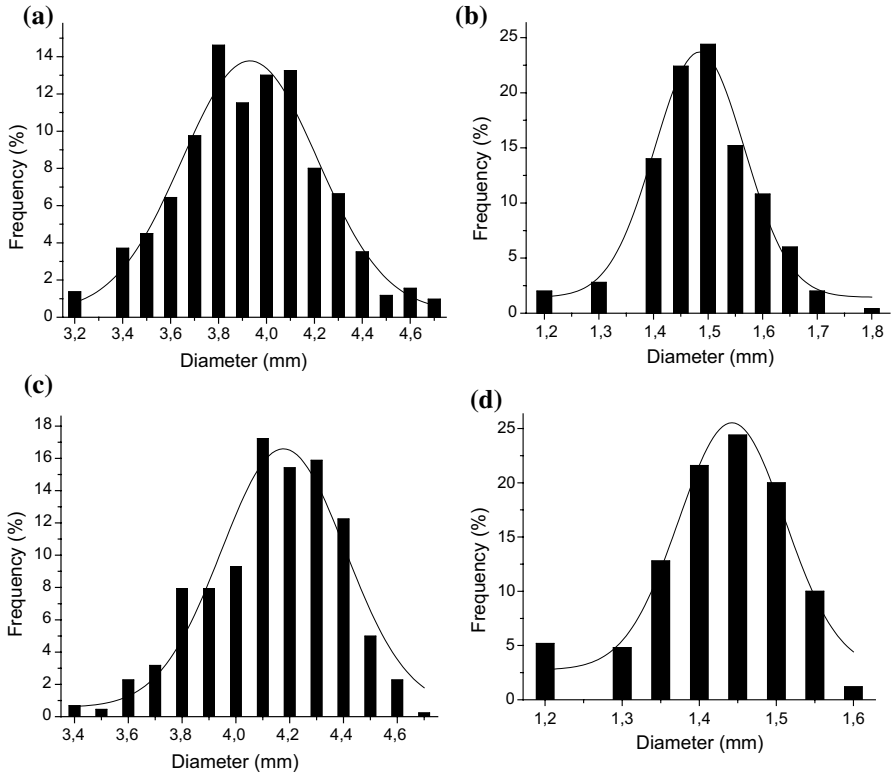

Fig. 4 Size distribution of different beads. **a** WCaAB, **b** DCaAB, **c** WEpAB and **d** DEpAB

Table 1 Average size and the polydispersity factor of different alginate beads

Beads	WCaAB	DCaAB	WEpAB	DEpAB
d_0 (mm)	3.93	1.48	4.17	1.44
σ	0.56	0.16	0.46	0.13

Table 2 Physico-chemical properties of the different beads

Beads	WCaAB	DCaAB	WEpAB	DEpAB
pH_{pzc}	7.91	7.99	7.84	7.66
Density (g mL^{-1})	1.0175	2.2285	1.0039	1.9334
W (%)	95 ± 0.2	–		–

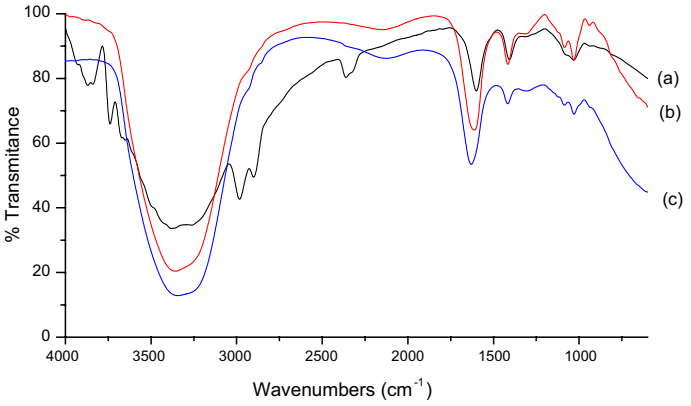

Fig. 5 FTIR spectra of **a** sodium alginate, **b** WCaAB and **c** WEpAB

different alginate beads are shown in Table 1. It should be noted that good reproducibility is obtained for the various syntheses as the results obtained demonstrate.

The physicochemical properties found for the different beads are summarized in Table 2 which indicates that the humidity ratio of the alginate beads cross-linked with epichlorohydrin is slightly higher than that of the calcium alginate beads, and this result is confirmed by the density values found. The pH_{pzc} values are approximately equal to 8 and less than 8 for calcium alginate beads and epichlorohydrin cross-linked alginate beads, respectively. So the adsorptive surface bead sites were positively charged under this pH_{pzc} and negatively charged over this pH level.

FTIR spectra of sodium alginate, WCaAB, and WEpAB are shown in Fig. 5. In the FTIR spectra of sodium alginate, the two bands at around 3382.53 cm^{-1} and 1031.73 cm^{-1} were assigned to –OH and C–O stretching vibrations, respectively, which indicates the presence of hydroxyl groups. The bands at 1600.63 cm^{-1} and 1407.78 cm^{-1} corresponding to C=O asymmetric and symmetric stretching vibrations of the carboxyl groups. The FTIR spectra of wet calcium alginate beads shows these two bands get shifted to 1612.2 cm^{-1} and 1415.49 cm^{-1},

respectively, revealing the occurrence of cross-linking between calcium ions and carboxyl group of sodium alginate, and in the FTIR spectra of wet epichlorohydrin cross-linked alginate beads, these same bands are shifted to 1629.55 cm^{-1} and 1417.42 cm^{-1}, respectively.

The surface morphology of calcium alginate beads and epichlorohydrin cross-linked alginate beads was studied by optical microscopy and SEM technique.

For the SEM technique, the micrographs of samples were recorded in the dried state. The SEM images of the surface of DCaAB and DEpAB are shown in Fig. 6 which displays a smooth structure on the surface with a large surface area. An examination of the SEM micrographs indicates the presence of ripples and also some cracks on the surface of beads probably caused by partial collapsing of the polymer network during drying.

The optical microscope was used to investigate the surface morphology of different beads before and after drying. The photographs of calcium alginate beads and epichlorohydrin cross-linked alginate beads in both wet and dry states are shown in Fig. 7a–d. After adsorption, the photograph of wet epichlorohydrin

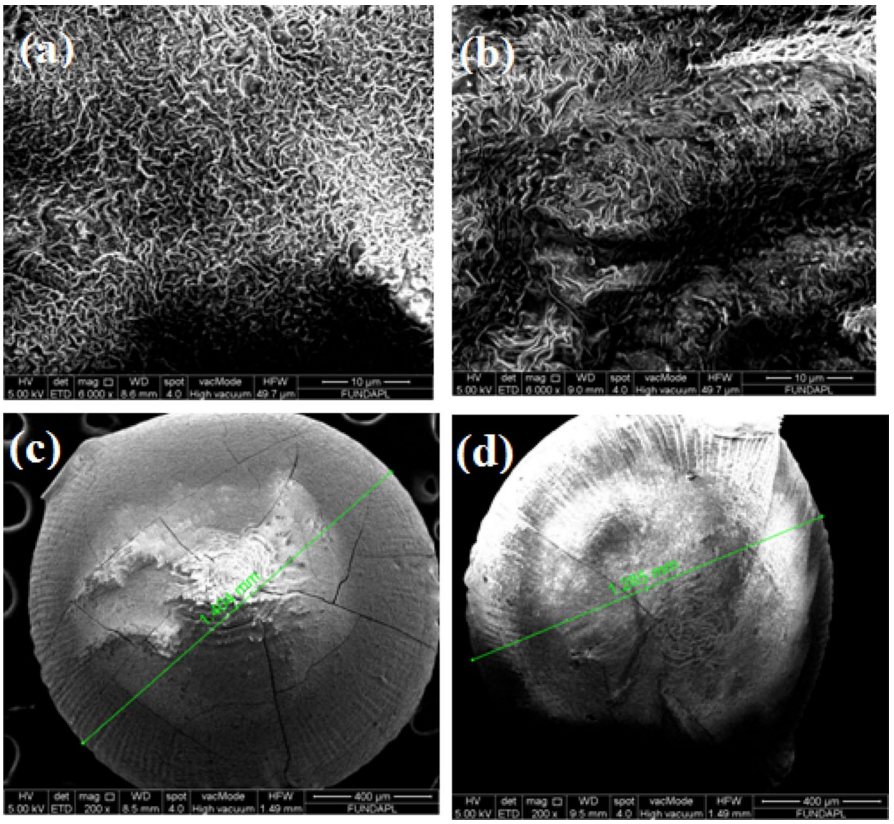

Fig. 6 SEM images of **a**, **c** DCaAB and **b**, **d** DEpAB

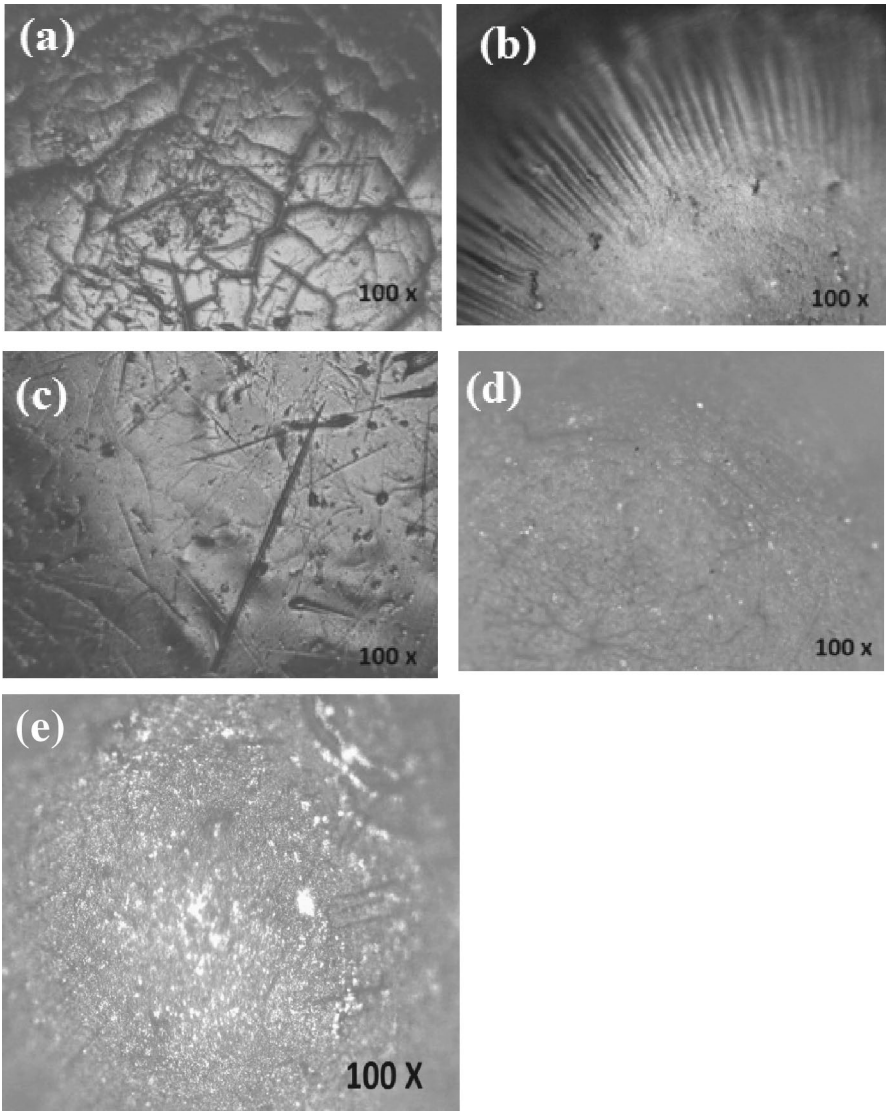

Fig. 7 Optical microscope photographs of **a** WCaAB, **b** DCaAB, **c** WEpAB and **d** DEpAB and DEpAB after adsorption

cross-linked alginate beads presented in Fig. 7e shows brightness on the surface of beads which is due to the presence and adsorption of methyl violet.

To confirm the cross-linking of alginate beads with epichlorohydrin, X-ray spectrometry analysis of the samples before and after chemical cross-linking was carried out. The spectra obtained are shown in Fig. 8. Analysis of the X-ray fluorescence spectrometry of calcium alginate beads and epichlorohydrin cross-linked alginate beads showed that the characteristic peak of calcium decreased after chemical

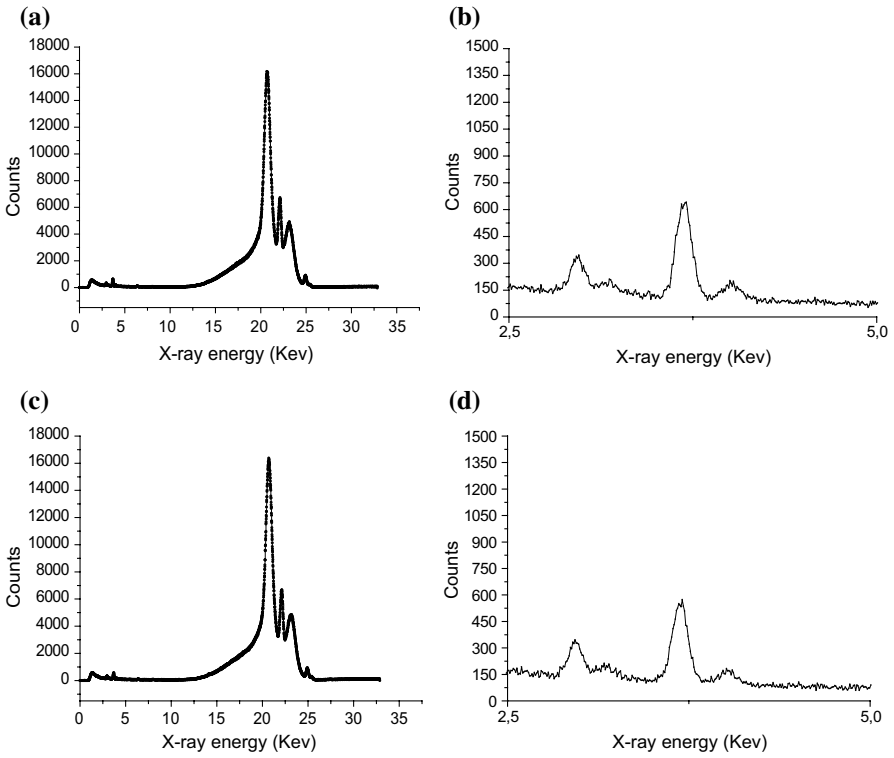

Fig. 8 **a**, **b** X-ray fluorescence spectrum of the calcium alginate beads (WCaAB). **c, d** X-ray fluorescence spectrum of epichlorohydrin cross-linked alginate beads (WEpAB)

cross-linking, and at the same time, the characteristic peak of C, H and O were increased. These results have demonstrated that the calcium ions were replaced by the epichlorohydrin molecules during the chemical cross-linking.

Adsorption studies

Effect of the nature of beads

Figure 9 shows the yields of removal of methyl violet depending on the nature of the pearls used.

Using the same conditions, the maximum percentages of MV elimination recorded for the different formulations of wet beads (WCaAB, WEpAB) are lower by a few orders magnitude (20–30%) to the elimination percentages of the same dye using the dried beads. This is related to the presence of a very large mass of water in the wet beads, weighing them down without contributing to the adsorption.

When compared with other alginate beads, the dry calcium alginate beads show a low adsorption capacity and a slowing of the adsorption kinetics. Indeed, after

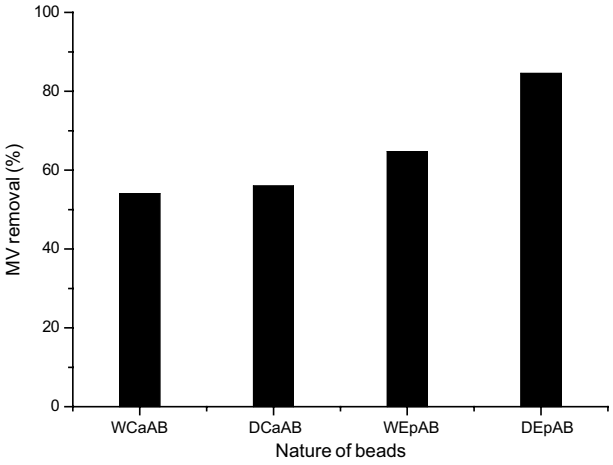

Fig. 9 Effect of the nature of beads on the MV percentage removal

drying, these beads (DCaAB) showed a significant loss of porosity leaving fears of a loss adsorption capacity.

Altering the cross-linking of the alginate matrix using epichlorohydrin makes the alginate gel elastic which allows dry beads to partially reinflate when placed in the solution. The dried alginate beads cross-linked with epichlorohydrin thus showed the best adsorption capacity, and they were kept and used for the further study of the adsorption.

Effect of contact time and initial MV concentration

The effect of contact time and initial dye concentration on MV removal was realized by varying the contact time from 0 to 5 h and varying the concentration of dye from 10 to 70 mg L^{-1} at pH 8. For this experiment, 2.5 g of dried beads (DEpAB) was employed with 100 ml of the dye solution and agitated at 300 rpm. The result is shown in Fig. 10, which indicates that from 0 to 180 min, the initial rate of dye uptake rapidly increased, due to the high availability of adsorption sites, and after this time, it leveled off. On the other hand, the % uptake shows a decreasing trend as the initial concentration of the dye is increased. At lower concentrations, all sorbate ions present in the adsorption medium could interact with the binding sites, hence resulting in higher % uptake. At higher concentrations, because of the saturation of the adsorption sites, the % uptake of the MV by the beads shows a decreasing trend.

Effect of amount of adsorbent (DEpAB)

In order to study the effect of the amount of adsorbent on MV removal, various amounts of alginate beads (DEpAB) were contacted with a fixed initial dye of 10 mg L^{-1}. The % uptake of MV after a contact time of 3 h versus the quantity of alginate beads used is shown in Fig. 11a. It could be observed from the figure

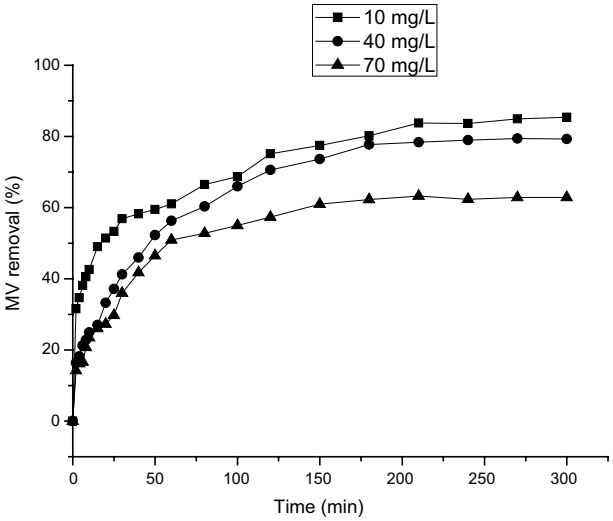

Fig. 10 Effect of contact time and initial MV concentration on the MV percentage removal

that the % uptake increased from 56.32 to 84.54% when the amount of beads was increased from 0.5 to 2.5 g respectively. Thus % uptake was maximum at the higher adsorbent amount. This could be attributed to the fact that as the adsorbent amount is increased, more adsorption sites are available for dye, thus enhancing the uptake. Also, with increasing adsorbent load, the quantity of dye adsorbed on to the unit weight of the adsorbent gets reduced, thus causing a decrease in Q_e value with increasing alginate loading.

Effect of stirring speed

The effect of the agitation removal of MV was studied with 100, 200, 300, 400, 500, and 700 stirrer rpm. The experiments were conducted with 10 mg L^{-1} initial concentration, 2.5 g of beads, initial pH 8 at room temperature. The effect of the stirring rate on the dye removal percentage is shown in Fig. 11b. As shown, the percentage removal of MV increases as the stirring rate of the system increases, indicating the occurrence of a stronger interaction between the beads and the dye. Furthermore, a higher removal percentage occurs when the stirring rate is equivalent to 300 rpm. For higher values, the percentage removal begins to decrease; the associated high rate of turbulence, in this case, might promote the entrainment of the MV particles before they can interact with the adsorbent.

Effect of pH

The pH of the aqueous solution is an important controlling parameter in adsorption because it influences not only the surface charge and the degree of ionization of the functional groups of the adsorbent, but also the dye chemistry [40, 41]. The

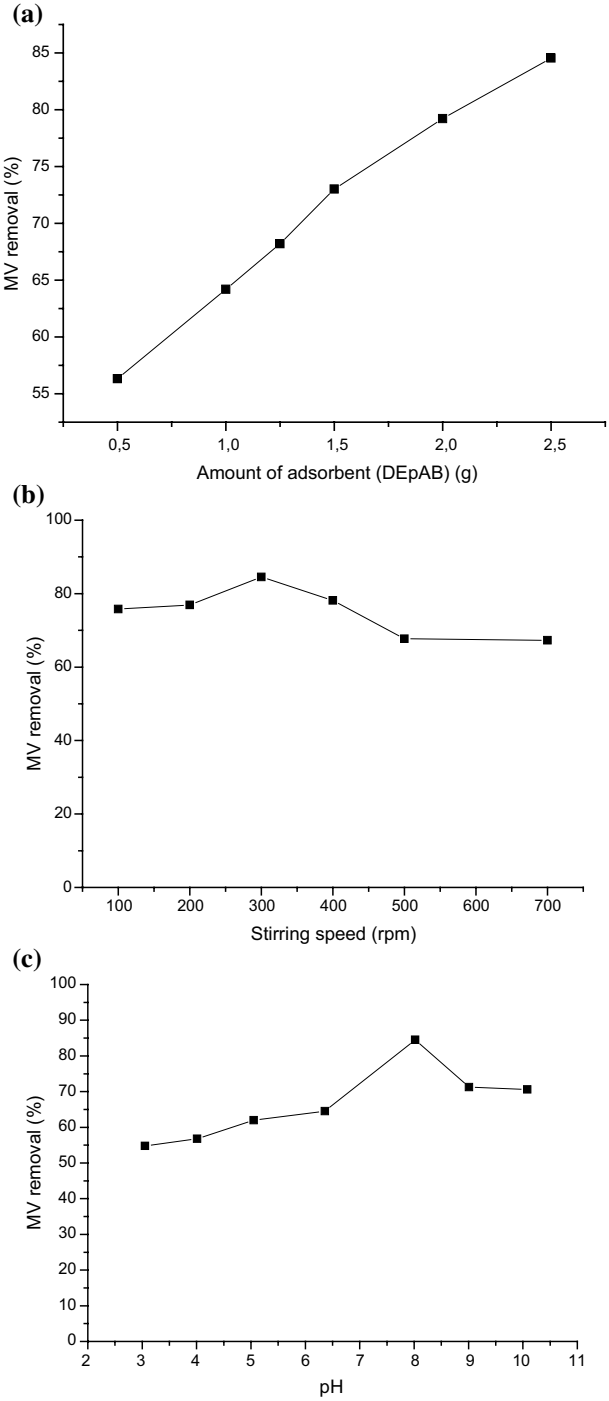

Fig. 11 Effects of amount of beads (DEpAB) (**a**), of stirring speed (**b**) and of pH (**c**) on the MV percentage removal

effect of pH on the dye (10 mg L^{-1}) removal was studied at the pH range from 3 to 10. The experiments were carried out at room temperature and 2.5 g of alginate beads (DEpAB). The acidity of the solution was adjusted using 0.1 M HCl and 0.1 M NaOH solutions. The effect of initial pH on dye removal is illustrated in Fig. 11c. It can be seen that adsorption was found to increase with the increase in pH dye solution up to pH 8 and decreased with further increase in pH of the dye solution. To determine the adsorption mechanism, measurement of zero point charge (pzc) of the adsorbent is crucial, since it is well known that adsorption of a cation is favorable at $pH > pH_{pzc}$ and for an anion, the favorable adsorption condition is $pH < pH_{pzc}$. Here we observed that the pH_{pzc} of alginate beads (DEpAB) is 7, 66. Therefore, in an acidic environment ($pH < pH_{pzc}$), a lower adsorption efficiency is expected because of the repulsive forces between the adsorbent and adsorbate. Additionally, an acidic pH and the increased surface excess of H^+ ions on the adsorbent imply completion of the H^+ ions with cationic dye molecules [42]. However, under alkaline conditions, the electrostatic attraction force increases, resulting in a higher % of adsorption of the cationic dye (MV) due to an increase in the amount of negatively charged sites. It explains that retention is more remarkable when the pH exceeds the value of 7.66; however, this loss of efficiency, at as the pH increases, shows that the reaction is rather complex and far from being a mere attraction electrostatic charge between opposite charge species. Elbariji et al. [43] reported that the primary alcohol functions of the cellulose and lignin, in the presence of NaOH, are transformed into alcoholic functions according to the following scheme.

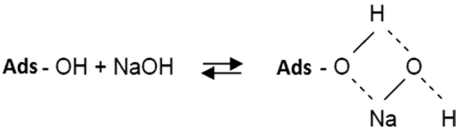

This hypothesis suggests that in the event that the medium becomes very basic, a competition is likely between the Na^+ cations of NaOH, smaller and more mobile than those of the dye (MV), thus preventing them from accessing the surface of the adsorbent.

Batch adsorption kinetic modeling

In this part, we will conduct investigations on the mechanism and on the rate controlling step in the overall adsorption process; for that, three kinetic models, pseudo-first-order, pseudo-second-order, and intra-particle diffusion models, are adopted to investigate the adsorption process. The pseudo-first-order and pseudo-second-order rate constants and correlation coefficients were calculated and are listed in Table 3.

For the pseudo-first-order, the values of the correlation coefficients R^2 obtained at all the studied concentrations are low. This suggests that this model is not suitable to describe the adsorption process.

The application of the intraparticle diffusion model does not give a straight line for all the concentration studied. Therefore, this model is not limiting the process of adsorption of MV on dry alginate beads (DAEpB).

Table 3 Kinetic constants for MV adsorption on dry alginate beads (DAEpB)

C_0 (mg L^{-1})	Experimental result Q_e (mg g^{-1})	Pseudo-first-order model			
		Equation	k_1 (min^{-1})	Q_e (mg g^{-1})	R^2
10	0.3208	$y=-0.007x-0.736$	0. 0161	0.1836	0.965
40	1.2437	$y=-0.007x+0.011$	0. 0161	1.0256	0.990
70	1.7437	$y=-0.009x+0.157$	0. 0207	1.4354	0.976
		Pseudo-second-order model			
		Equation	k_2 (g mg^{-1} min^{-1})	Q_e (mg g^{-1})	R^2
10	0.3208	$y=2.840x+43.56$	0. 187	0.35	0.994
40	1.2437	$y=0.719x+19.41$	0. 026	1.39	0.994
70	1.7437	$y=0.525x+11.08$	0. 025	1.90	0.996

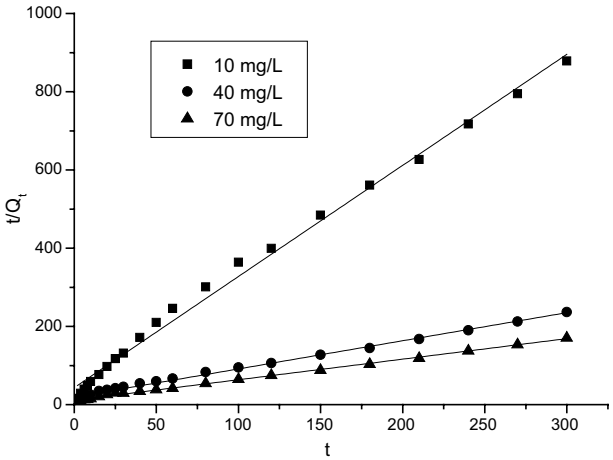

Fig. 12 Pseudo-second order model for batch adsorption of MV on dry alginate beads (DAEpB)

On the other hand, the good linear plots of t/Q_t versus t (Fig. 12) at different concentrations with the correlation coefficients R^2 higher than 0.99 suggest that adsorption of MV onto the dry alginate beads (DAEpB) predominantly follow the pseudo-second-order kinetic model. Moreover, with this model, the equilibrium sorption capacities show a good agreement with the experimental values.

Conclusion

In this study, alginate beads were prepared by an extrusion dripping method using physical and chemical cross-linking and characterized by FTIR, optical microscopy, SEM, and X-ray fluorescence. These beads were developed in an attempt to

selectively remove organic compounds from wastewater. Sorption experiments were performed using methyl violet as a model of pollutant. Comparative study of adsorption was conducted with alginate beads cross-linked by Ca^{2+} ions or epichlorohydrin in a dry or wet state to evaluate the adsorption capacity. It has been shown that the use of epichlorohydrin in a dry state gives the best removal of methyl violet. The effect of different parameters such as pH, sorbent amount, contact time, sorbate concentration, and the stirring speed was studied. The pseudo-second-order kinetic model adequately describes the experimental data. Results showed that alginate beads can be effectively used as a low-cost and eco-friendly adsorbent for removal of dye in aqueous solution.

References

1. Ya-Fen L, Hua-Wei C, Poh-Sun C, Chyow-San C, Cheng-Chung L (2011) Application of bifunctional magnetic adsorbent to adsorb metal cations and anionic dyes in aqueous solution. J Hazard Mater 185:1124–1130
2. Ting L, Tao X, Xue-Lian H, Cheng L, Wei-Feng Z, Qian Z, Chang-Sheng Z (2015) Post-crosslinking towards stimuli-responsive sodium alginate beads for the removal of dye and heavy metals. Carbohydr. Polym. 133:587–595
3. Crini G (2006) Non-conventional low-cost adsorbents for dye removal: a review. Biores Technol. 97:1061–1085
4. Pearce CI, Lloyd JR, Guthrie JT (2003) The removal of colour from textile wastewater using whole bacterial cells: a review. Dyes Pigments 58:179–196
5. Tan IAW, Hameed BH, Ahmad AL (2007) Equilibrium and kinetic studies on basic dye adsorption by oil palm fibre activated carbon. Chem. Eng. J. 127:111–119
6. Raffainer II, Rudolf von Rohr P (2001) Promoted wet oxidation of the azo dye Orange II under mild conditions. Ind. Eng. Chem. Res. 40:1083–1089
7. Elwakeel KZ, El-Bindary AA, El-Sonbati AZ, Hawas AR (2017) Magnetic alginate beads with high basic dye removal potential and excellent regeneration ability. Rev. Can. Chim. 95(8):807–815
8. Shojaat R, Saadatjoo N, Karimi A, Aber S (2016) Simultaneous adsorption–degradation of organic dyes using $MnFe_2O_4$/calcium alginate nano-composites coupled with GOx and laccase. J. Environ. Chem. Eng. 4:1722
9. Ali I, Gupta VK (2007) Advances in water treatment by adsorption technology. Nat. Protoc. 1:2661
10. Subbaiah MV, Kim DS (2016) Adsorption of methyl orange from aqueous solution by aminated pumpkin seed powder: kinetics, isotherms, and thermodynamic studies. Ecotoxicol. Environ. Saf. 128:109
11. Lakshmipathy R, Sarada NC (2016) Methylene blue adsorption onto native watermelon rind: batch and fixed bed column studies. Desalin. Water. Treat. 57:10632
12. Al-Kahtani AA, Abou Taleb MF (2016) Photocatalytic degradation of Maxilon CI basic dye using CS/$CoFe_2O_4$/GONCs as a heterogeneous photo-Fenton catalyst prepared by gamma irradiation. J. Hazard. Mater. 309:10–19
13. Vaiano V, Iervolino G, Sannino D, Murcia JJ, Hidalgo MC, Ciambelli P, Navío JA (2016) Photocatalytic removal of patent blue V dye on Au–TiO_2 and Pt–TiO_2 catalysts. Appl. Catal. B 188:134–146
14. Thangavel S, Thangavel S, Raghavan N, Krishnamoorthy K, Venugopal G (2016) Visible-light driven photocatalytic degradation of methylene-violet by rGO/Fe_3O_4/ZnO ternary nanohybrid structures. J. Alloys Compd. 665:107
15. Aravind P, Subramanyan V, Ferro S, Gopalakrishnan R (2016) Eco-friendly, and facile integrated biological-cum-photo assisted electrooxidation process for degradation of textile wastewater. Water Res. 93:230
16. Benjwal P, Kar KK (2015) Removal of methylene blue from waste water under low power irradiation source by Zn, Mn co-doped TiO_2 photocatalyst. RSC Adv. 5:98166
17. Papic S, Koprivanac N, Bozic AL, Metes A (2004) Removal of some reactive dyes from synthetic wastewater by combined Al(III) coagulation/carbon adsorption process. Dyes Pigments 62:291
18. Bouras HD, Benturki O, Bouras N, Attou M, Donnot A, Merlin A, Addoun F, Holtz MD (2015) The use of an agricultural waste material from *Ziziphus jujuba* as a novel adsorbent for humic acid removal from aqueous solutions. J. Mol. Liq. 211:1039–1046

19. Baban A, Yediler A, Lienert D, Kemerdere N, Kettrup A (2003) Ozonation of high strength segregated effluents from a woollen textile dyeing and finishing plant. Dyes Pigments 58:93
20. Xu L, Sun Y, Zhang L, Zhang J, Wang F (2015) Electrochemical oxidation of C.I. Acid Red 73 wastewater using Ti/SnO_2–Sb electrodes modified by carbon nanotube. Desalin. Water. Treat. 57:8815–8825
21. Edip B, Erol A (2010) Electrochemically enhanced removal of polycyclic aromatic basic dyes from dilute aqueous solutions by activated carbon cloth electrodes. Environ. Sci. Technol. 44:6331–6336
22. Ledakowicz S, Solecka M, Zylla R (2001) Biodegradation, decolourisation and detoxification of textile wastewater enhanced by advanced oxidation processes. J. Biotechnol. 89:175
23. Tan BH, Teng TT, Mohd Omar AKM (2000) Removal of dyes and industrial dye wastes by magnesium chloride. Water Res. 34:597–601
24. Koyuncu I, Topacik D, Yuksel E (2004) Reuse of reactive dye house wastewater by nanofiltration: process water quality and economical implications. Sep. Purif. Technol. 36:77–85
25. Slejko FL (1985) Adsorption Technology: A Step-by-step Approach to Process Evaluation and Application. Marcel Dekker, New York
26. Hasan S, Krishnaiah A, Ghosh TK, Viswanath DS (2006) Adsorption of divalent cadmium (Cd(II)) from aqueous solutions onto chitosan-coated perlite beads. Ind. Eng. Chem. Res. 45:5066–5077
27. Huang GL, Zhang HY, Shi JX, Langrish TAG (2009) Adsorption of chromium(VI) from aqueous solutions using cross-linked magnetic chitosan beads. Ind. Eng. Chem. Res. 48:2646–2651
28. Kumar NS, Suguna M, Subbaiah MV, Reddy AS, Kumar NP, Krishnaiah A (2010) Adsorption of phenolic compounds from aqueous solutions onto chitosan-coated perlite beads as biosorbent. Ind. Eng. Chem. Res. 49:9238–9247
29. Rocher V, Siaugue J-M, Cabuil V, Bee A (2008) Removal of organic dyes by magnetic alginate beads. Water Res. 42:1290–1298
30. Fundueanu G, Nastruzzi C, Carpov A, Desbrieres J, Rinaudo M (1999) Physico-chemical characterization of Ca-alginate microparticles produced with different methods. Biomaterials 20:1427–1435
31. Blandino A, Macias M, Cantero D (1999) Formation of calcium alginate gel capsules: influence of sodium alginate and $CaCl_2$ concentration on gelation kinetics. J. Biosci. Bioeng. 88(6):686–689
32. Rocher V, Bee A, Siaugue J-M, Cabuil VE (2010) Dye removal from aqueous solution by magnetic alginate beads crosslinked with epichlorohydrin. J. Hazard. Mater. 178:434–439
33. Zhao W, Wahyu R, Nugroho N, Odelius K, Edlund U, Zhao C, Albertsson AC (2015) In situ crosslinking of stimuli-responsive hemicellulose microgels during spray drying. CS Appl. Mater. Interfaces 7(7):4202–4215. https://doi.org/10.1021/am5084732
34. Zhao W, Odelius K, Edlund U, Zhao C, Albertsson AC (2015) In situ synthesis of magnetic field-responsive hemicellulose hydrogels for drug delivery. Biomacromolecules 16(8):2522–2528. https://doi.org/10.1021/acs.biomac.5b00801
35. Vijayakumar G, Dharmendirakumar M, Renganathan S, Sivanesan S, Baskar G, Elango KP (2009) Removal of congo red from aqueous solutions by perlite. Clean-Soil Air Water 37:355–364
36. Ho Y, McKay G (1999) Pseudo-second order model for sorption processes. Process Biochem. 34:451–465
37. Weber WJ, Morris JC (1963) Kinetics of adsorption on carbon from solution. Eng. Div. Proc. Am. Soc. Civil Eng. 89:31–60
38. Smidsrod O (1974) Molecular basis for some physical properties of alginate in gel state. Faraday Discuss. Chem. Soc. 57:263
39. Bhattarai N, Zhang MQ (2007) Controlled synthesis and structural stability of alginate-based nanofibers. Nanotechnology. https://doi.org/10.1088/0957-4484/18/45/455601
40. Gupta VK, Jain R, Varshney S, Saini VK (2007) Removal of Reactofix Navy Blue 2 GFN from aqueous solution using adsorption techniques. Colloid. Interface Sci. 307:326–332
41. Meenakshi Sundaram M, Sivakumar S (2012) Use of Indian almond shell waste and groundnut shell waste for the removal of azure A dye from aqueous solution. J. Chem. Pharm. Res. 4:2047–2054
42. Crini G, Peindy HN, Gimbert F, Robert C (2007) Removal of CIBasic Green 4 (Malachite Green) from aqueous solutions by adsorption using cyclodextrin-based adsorbent: kinetic and equilibrium studies. Sep. Purif. Technol. 53:97–110
43. Elbariji S, Elamine M, Eljazouli H, Kabli H, Lacherai A, Albourine A (2006) Traitement et valorisation des sous-produits du bois. Application à l'élimination des colorants industriels. C.R. Chimie 9:1314–1321

Affiliations

Akila Merakchi[1,2] · Souhila Bettayeb[2,3] · Nadjib Drouiche[4] · Lydia Adour[5] · Hakim Lounici[2,6]

[1] Département de Chimie, Faculté des Sciences, Université Mouloud Mammeri, Tizi Ouzou, Algeria

[2] MDD Lab, Université Akli Mohand Oulhadj, Bouira, 10000 Bouira, Algeria

[3] Ecole Nationale Polytechnique, 10 Hassen Badi, El Harrach, 16200 Alger, Algeria

[4] CRSTE, Centre de Recherche en Technologie des Semi-conducteurs pour l'Energétique, 2, Boulevard Frantz Fanon, Alger BP 140 Alger-7 Merveilles, 16038 Alger, Algeria

[5] Université d'Alger1, 2 Rue Didouche Mourad, Alger Centre, 16000 Algiers, Algeria

[6] CRAPC, Centre de Recherche en Analyses Physico-Chimiques, BP 384, Z.I. Bou-Ismail CP, 42004 Tipaza, Algeria